

has recently been suggested by Feller and McQuarrie;⁴ their variational solution of the integral equation theory⁴ seems to offer both reasonable accuracy and computational simplicity. To our knowledge, with the exception of the preliminary results reported in refs 7 and 33, no numerical data based on the solution of the

integral equation theories for the cylindrical micropores have been published so far.

Acknowledgment. The support of the Research Community of Slovenia is gratefully acknowledged. The authors thank Dr. Dirk Stigter and Stephen Lambert for critical reading of the manuscript.

(45) Outhwaite, C. W. *J. Chem. Soc., Faraday Trans. 2* 1986, 82, 789.

Aminoalkyl and Alkylaminium Free Radicals and Related Species: Structures, Thermodynamic Properties, Reduction Potentials, and Aqueous Free Energies

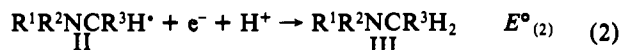
David A. Armstrong,* Arvi Rauk,* and Dake Yu

Contribution from the Department of Chemistry, The University of Calgary, Calgary, Alberta, Canada T2N 1N4. Received July 14, 1992

Abstract: The structures of H_2NCH_2^+ , $\text{H}_2\text{NCH}_2^\cdot$, H_2NCH_3 , $\text{H}_2\text{NCH}_3^{++}$, H_3NCH_2^+ , $(\text{CH}_3)_2\text{NCH}_2^+$, $(\text{CH}_3)_2\text{NCH}_2^\cdot$, $(\text{CH}_3)_3\text{N}$, and $(\text{CH}_3)_3\text{N}^{++}$ were optimized at the HF/6-31G* and MP2/6-31+G* levels, and the frequencies were calculated at the HF/6-31G* level. For H_2NCH_2^+ , $\text{H}_2\text{NCH}_2^\cdot$, H_2NCH_3 , $\text{H}_2\text{NCH}_3^{++}$, and H_3NCH_2^+ the total energies were evaluated at the G2 level and those of $(\text{CH}_3)_2\text{NCH}_2^+$, $(\text{CH}_3)_2\text{NCH}_2^\cdot$, $(\text{CH}_3)_3\text{N}$, and $(\text{CH}_3)_3\text{N}^{++}$ at the level of MP2/6-31+G*+ZPE. Where comparisons were possible, heats of formation from these results agreed well with recent literature data. On the basis of the structural information from the ab initio calculations and an analysis of the solution free energies of the parent compounds, solution free energies were calculated for the radicals studied by the G2 procedure and several others for which reliable heats of formation were available. These data were used to obtain values of $\Delta_f G^\circ(\text{aq})$ and reduction potentials for the $\text{R}^1\text{R}^2\text{NCR}^3\text{H}^\cdot$ radicals in reaction 2: $\text{R}^1\text{R}^2\text{NCR}^3\text{H}^\cdot + e^- + \text{H}^+ \rightarrow \text{R}^1\text{R}^2\text{NCR}^3\text{H}_2$. The values of $\Delta_f G^\circ(\text{aq})$ for several ionic species were obtained from literature data and used to calculate values of $E^\circ_{(6)}$ for reaction 6: $\text{R}^1\text{R}^2\text{NCR}^3\text{H}_2^{++} + e^- \rightarrow \text{R}^1\text{R}^2\text{NCR}^3\text{H}_2$. Estimates of $E^\circ_{(1)}$ for reaction 1, $\text{R}^1\text{R}^2\text{NCR}^3\text{H}^+ + e^- \rightarrow \text{R}^1\text{R}^2\text{NCR}^3\text{H}^\cdot$, were also obtained. These confirmed the strong reducing character of the α -amino radicals. Existing experimental data on aqueous solutions are discussed in the light of the present results.

1. Introduction

Apart from their intrinsic interest in organic chemistry, α -carbon-centered and nitrogen-centered free radicals of amines are of practical importance in several areas. For example, they have been postulated as intermediates in the photochemistry of nitrosamines¹ and in the reaction mechanisms of some amine oxidases,^{2,3} and they are frequently used in biological chemistry as reducing agents.⁴ The same radicals are probably also involved when amines are used as sacrificial hydrogen donors in redox systems activated by solar energy.⁵ Typical redox reactions which have been proposed⁶ are written below for a generalized radical, $\text{R}^1\text{R}^2\text{NCR}^3\text{H}^\cdot$, with R^1 , R^2 , and R^3 representing organic groups or H atoms. The radical II is seen to be the intermediate redox form between the iminium I and the amine III. The second



reaction probably occurs sequentially, with prior protonation followed by rapid electron transfer. Experimental work^{6,7} has shown that II is protonated to form the N-centered radical IV:

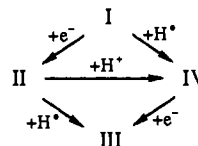


rather than the C-centered radical V



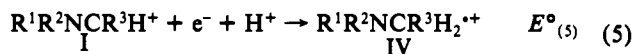
In the above, and in subsequent equations for reactions, we indicate

Scheme I

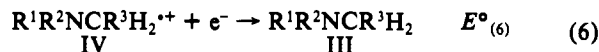


the quantities of interest which will be evaluated. For example, $E^\circ_{(1)}$ is the reduction potential in aqueous solution for reaction 1 and $\Delta G^\circ_{(3)}$ is the free energy change for reaction 3.

There are two other redox reactions that must be considered:



and



(1) Chow, Y. L. *Acc. Chem. Res.* 1973, 6, 354.

(2) Singer, T. P.; Van Korff, R. W.; Murphy, D. L., Eds. *Monamine Oxidase: Structure, Function, and Altered Functions*; Academic Press: New York, 1979.

(3) (a) Silverman, R. B.; Hoffman, S. J. *J. Am. Chem. Soc.* 1980, 102, 884. (b) Simpson, J. T.; Krantz, A.; Lewis, F. D.; Kokel, B. *J. Am. Chem. Soc.* 1982, 104, 7155.

(4) See, for example: Armstrong, J. S.; Hemmerich, P.; Traber, R. *Photochem. Photobiol.* 1982, 35, 747 and references therein.

(5) Hoffman, M. Z. *J. Phys. Chem.* 1988, 92, 3458.

(6) Chow, Y. L.; Danen, W. C.; Nelsen, S. F.; Rosenblatt, D. H. *Chem. Rev.* 1978, 78, 243.

(7) Das, S.; von Sonntag, C. Z. *Naturforsch.* 1986, 41b, 505. Das, S.; Schuchmann, M. N.; Schuchmann, H.-P.; von Sonntag, C. *Chem. Ber.* 1987, 120, 319.

* The authors to whom correspondence should be addressed.

Equations 1–6 can be summarized by Scheme I. The practical importance of these species in aqueous reaction systems means that the structures and thermodynamic properties of the reactants and products are of considerable interest. While amines are stable and relatively well studied, there is much less information available for the amine radicals, and also for the iminium cations, which are normally unstable—particularly in aqueous solution.^{6,8} Measurements of $E^\circ_{(6)}$, the reduction potentials for reaction 6, with amines possessing radical-stabilizing substituents have been reported in various nonaqueous solvents,^{6,9} and a few measurements have been made in water.^{6,10} However, often even the values for the reduction potential $E^\circ_{(6)}$ in nonaqueous solvents cannot be obtained under reversible conditions, and almost nothing is known about the free energy changes or E° values for the other reactions. For the simpler amines with short-lived radicals, thermodynamic data in aqueous solution are generally not available. In these circumstances, the calculation of $\Delta_r G^\circ(\text{aq})$ and E° values from the gas-phase thermodynamic properties of the amines and their free radicals can be of great assistance.

For the above reasons we have made use of the extensive gas-phase thermodynamic data¹¹ for the amines and their free radicals to calculate solution thermodynamic properties and the reduction potentials for $\text{R}^1\text{R}^2\text{NCR}^3\text{H}^\bullet$ and $\text{R}^1\text{R}^2\text{NCR}^3\text{H}_2^{+\bullet}$ radicals derived from methylamine, ethylamine, dimethylamine, and trimethylamine. The procedure requires a knowledge of the structures of the species involved. Thus modern ab initio molecular orbital methods were used to obtain these structures for the amines and radicals with $\text{R}^1 = \text{R}^2 = \text{H}$, $\text{R}^3 = \text{H}$ and $\text{R}^1 = \text{R}^2 = \text{CH}_3$, $\text{R}^3 = \text{H}$. The computational details have been given in section 2. In section 3 we report the computational results and discuss the general features. We introduce the gas-phase thermochemical data in section 4 and use this information and thermochemical data from the literature to calculate reduction potentials and aqueous free energies of formation of several of the species occurring in reactions 1–6 for methylamine, ethylamine, dimethylamine, and trimethylamine. The results of the present study are discussed in conjunction with those of earlier experimental and theoretical investigations. It should be pointed out that these include a number of investigations which have been made by ab initio methods. As in the present study, these have led to heats of formation accurate to within a few 10's of kJ mol^{-1} as well as structural information.

2. Computational Details

Ab Initio Calculations. All ab initio calculations presented here were performed with the Gaussian 90¹² molecular orbital package. For $\text{H}_2\text{NCH}_2^\bullet$, $\text{H}_2\text{NCH}_2^\bullet$, H_2NCH_3 , $\text{H}_2\text{NCH}_3^{+\bullet}$, and $\text{H}_3\text{NCH}_2^{+\bullet}$, it is possible to evaluate their energies at the G2 level.¹³ The G2 procedure includes a geometry optimization with the standard Hartree–Fock (HF) method and the 6-31G* split-valence basis set (HF/6-31G*); a vibrational frequency calculation at the HF optimized geometry; the second-order Moller–Plesset (MP2) optimization with the 6-31G* basis set; and a series of single-point post-HF calculations carried out on the MP2 optimized geometries to obtain an accurate evaluation of the correlation energies. For the di- and trimethyl derivatives, $(\text{CH}_3)_2\text{NCH}_2^\bullet$, $(\text{CH}_3)_2\text{NCH}_2^\bullet$, $(\text{CH}_3)_3\text{N}$, and $(\text{CH}_3)_3\text{N}^{+\bullet}$, the geometries were first optimized at HF/6-31G* levels and the vibrational frequencies were calculated. The optimizations were then carried

out at MP2/6-31+G* to include the diffuse functions which are important for species with nonbonded electrons and to provide an estimation of the correlation effects on the geometries. In considering the contribution to the total energies from the vibrational zero-point energies (ZPE) and in calculating the thermodynamic functions, the vibrational frequencies were scaled by a factor of 0.89 to take into account known inadequacies in frequencies calculated at the HF level.¹⁴ In order to compare structural characteristics of the methyl-substituted molecules with those of the parent compounds, the geometries of $\text{H}_2\text{NCH}_2^\bullet$, $\text{H}_2\text{NCH}_2^\bullet$, H_2NCH_3 , $\text{H}_2\text{NCH}_3^{+\bullet}$, and $\text{H}_3\text{NCH}_2^{+\bullet}$ were also optimized at the MP2 level with the 6-31+G* basis set.

Thermodynamic Properties. Ideal gas thermodynamic functions, C_p° , S° , and $H^\circ - H^\circ_0$, in the temperature range 0–298.15 K and 1 bar of pressure were computed for all of the species listed in the preceding section by standard statistical thermodynamic methods, on the basis of the rigid rotor–harmonic oscillator model and using the frequencies obtained at the HF/6-31G* level. The computed vibrational frequencies were scaled by a factor of 0.89 in calculating the vibrational contributions to the above thermodynamic functions. Heats of formation at 0 K for $\text{H}_2\text{NCH}_2^\bullet$, $\text{H}_2\text{NCH}_2^\bullet$, H_2NCH_3 , $\text{H}_2\text{NCH}_3^{+\bullet}$, and $\text{H}_3\text{NCH}_2^{+\bullet}$ were calculated directly from the G2 energies and compared with those derived by using an experimental value (if available) at one reference temperature. The calculated values of $H^\circ - H^\circ_0$ were used to evaluate heats of formation at other temperatures. For the other systems, experimental heats of formation and, where available, values of $\Delta_r G^\circ_{298}$ and S°_{298} were taken from the literature. Where these were not available, the values of S°_{298} were calculated by utilizing the additivity relationships of Benson et al.¹⁵ Values of $\Delta_r G^\circ_{298}$ were then derived from the experimental values of $\Delta_r H^\circ_{298}$ and the entropy change of the formation reaction for each substance. The values of S°_{298} for the elements were taken from Wagman et al.¹⁶

3. Computational Results and Discussion

Equilibrium Structures. The structures for $\text{H}_2\text{NCH}_2^\bullet$, $\text{H}_2\text{NCH}_2^\bullet$, H_2NCH_3 , $\text{H}_2\text{NCH}_3^{+\bullet}$, $\text{H}_3\text{NCH}_2^{+\bullet}$, $(\text{CH}_3)_2\text{NCH}_2^\bullet$, $(\text{CH}_3)_2\text{NCH}_2^\bullet$, $(\text{CH}_3)_3\text{N}$, and $(\text{CH}_3)_3\text{N}^{+\bullet}$ optimized at the MP2/6-31+G* level are shown in Figure 1 with a few characteristic parameters listed. The full geometric parameters in the Z-matrix format are submitted as supplementary data. The total energies calculated at the MP2/6-31+G*+ZPE and G2 levels for $\text{H}_2\text{NCH}_2^\bullet$, $\text{H}_2\text{NCH}_2^\bullet$, H_2NCH_3 , $\text{H}_2\text{NCH}_3^{+\bullet}$, and $\text{H}_3\text{NCH}_2^{+\bullet}$ and at the MP2/6-31+G*+ZPE level for $(\text{CH}_3)_2\text{NCH}_2^\bullet$, $(\text{CH}_3)_2\text{NCH}_2^\bullet$, $(\text{CH}_3)_3\text{N}$, and $(\text{CH}_3)_3\text{N}^{+\bullet}$ are presented in Table I. Also listed in Table I are the spin and charge (with the charges on the hydrogen atoms summed into the heavy ones) distributions on the heavy atoms. The general features of HF and MP2 geometries are qualitatively the same. The MP2 results are discussed specifically below.

The iminium cation, H_2NCH_2^+ , is planar with C_{2v} symmetry. The corresponding aminomethyl radical, $\text{H}_2\text{NCH}_2^\bullet$, is pyramidal at both N and C and has a staggered arrangement of bonds to hydrogen and C_s symmetry. The out-of-plane angle γ_N (angle formed by the HNH plane and the C–N bond) is 42.1° , essentially the same as that obtained by UHF/6-31G*, 46.4° , and not much different from the pyramidal angle calculated for H_2NCH_3 , 53.3° (experimental value,¹⁷ 54.3°). The aminomethyl radical is also pyramidal at carbon with the out-of-plane angle at C, $\gamma_C = 32.4^\circ$. The optimized C–N bond length of the radical is 1.399 Å, intermediate in length between the C–N bonds in the iminium cation, H_2NCH_2^+ (1.282 Å), and methylamine, H_2NCH_3 (1.466 Å; observed value¹⁷ 1.4714 Å).

(8) Iminium cations are readily hydrolyzed to carbonyl species.

(9) Smith, J. R. L.; Masheder, D. *J. Chem. Soc., Perkin Trans. 2* 1976, 47.

(10) Hawari, J. A.; Kanabus-Kaminska, J. M.; Wayner, D. D. M.; Griller, D. *Substituent Effects in Radical Chemistry*; Vieh, H. G., et al., Eds.; D. Reidel Publ. Co.: Norwell, MA, 1986; 91.

(11) Lias, S. G.; Bartmess, J. E.; Liebman, J. F.; Holmes, J. L.; Levin, R. D.; Mallard, W. G. *J. Phys. Chem. Ref. Data* 1988, 17, Suppl. No. 1.

(12) Frisch, M. J.; Head-Gordon, M.; Trucks, G. W.; Foresman, J. B.; Schlegel, H. B.; Raghavachari, K.; Robb, M. A.; Binkley, J. S.; Gonzalez, C.; Defrees, D. J.; Fox, D. J.; Whiteside, R. A.; Seeger, R.; Mellus, C. F.; Baker, J.; Martin, R. L.; Kahn, L. R.; Stewart, J. J. P.; Topiol, S.; Pople, J. A. *Gaussian 90*; Gaussian, Inc.: Pittsburgh, PA, 1990.

(13) Curtiss, L. A.; Raghavachari, K.; Trucks, G. W.; Pople, J. A. *J. Chem. Phys.* 1991, 94, 7221.

(14) Pople, J. A.; Schlegel, H. B.; Krishnan, R.; Defrees, K. J.; Binkley, J. B.; Frisch, M. J.; Whiteside, R. A.; Hout, R. F.; Hehre, W. J. *Int. J. Quantum Chem. Symp.* 1981, 15, 269.

(15) Benson, S. W. *Thermochemical Kinetics*, 2nd ed.; Wiley: New York, 1976.

(16) Wagman, D. D.; Evans, W. H.; Parker, V. B.; Schumm, R. H.; Halow, I.; Bailey, S. M.; Churney, K. L.; Nuttall, R. L. *J. Phys. Chem. Ref. Data* 1982, 11, Suppl. No. 2.

(17) Takagi, K.; Kojima, T. *J. Phys. Soc. Jpn.* 1971, 30, 1145.

Table I. Total Energies and Charge and Spin Distributions on the Heavy Atoms

	$E(\text{MP2/6-31+G}^*)$ (hartrees)	ZPE ^a (hartrees)	$E(\text{G2})$ (hartrees)	$\langle S^2 \rangle$		charge ^b	spin
H_2NCH_2^+	-94.669 962	0.058 440	-94.791 844	0.00	N	0.305	
					C	0.695	
$\text{H}_2\text{NCH}_2^\bullet$	-94.750 523	0.053 854	-95.025 190	0.76	N	-0.115	0.260
					C	0.115	1.328
H_2NCH_3	-95.523 819	0.068 911	-95.666 910 ^c	0.00	N	-0.168	
					C	0.168	
$\text{H}_2\text{NCH}_3^{++}$	-95.201 300	0.066 540	-95.332 675	0.76	N	0.538	1.305
					C	0.462	-0.076
$\text{H}_3\text{NCH}_2^{++}$	-95.207 943	0.068 422	-95.334 276	0.76	N	0.599	-0.084
					C	0.401	1.368
$(\text{CH}_3)_2\text{NCH}_2^+$	-173.030 543	0.119 170		0.00	N	-0.029	
					C	0.405	
					C	0.312	
					C	0.312	
$(\text{CH}_3)_2\text{NCH}_2^\bullet$	-173.213 163	0.114 685		0.76	N	-0.200	0.299
					C	-0.019	1.512
					C	0.110	-0.007
					C	0.110	-0.007
$(\text{CH}_3)_3\text{N}$	-173.857 773	0.129 505		0.00	N	-0.279	
					C	0.093	
					C	0.093	
					C	0.093	
$(\text{CH}_3)_3\text{N}^{++}$	-173.575 989	0.127 900		0.77	N	0.076	1.475
					C	0.308	-0.089
					C	0.308	-0.089
					C	0.308	-0.089

^a HF/6-31G* level. ^b Charges on the hydrogens summed into heavy atoms. ^c From ref 13.

Comparison of the two related radical cations, $\text{H}_2\text{NCH}_3^{++}$ and $\text{H}_3\text{NCH}_2^{++}$, is of special interest. The former is a nitrogen-centered radical cation substituted by CH_3 , while the latter is a carbon-centered radical with an NH_3^+ substituent. The C–N bond is substantially shorter in $\text{H}_2\text{NCH}_3^{++}$ (1.430 Å) than in $\text{H}_3\text{NCH}_2^{++}$ (1.469 Å), indicating significantly greater involvement of the methyl group in bonding of the NH_2^{++} center than the contribution of the quaternary nitrogen to the bonding at the carbon radical. The nitrogen-centered radical site in $\text{H}_2\text{NCH}_3^{++}$ is almost planar, with an out-of-plane angle $\gamma_N = 3.2^\circ$. The corresponding out-of-plane angle is much larger for the carbon-centered radical $\text{H}_3\text{NCH}_2^{++}$, $\gamma_C = 17.4^\circ$.

The dimethyliminium cation, $(\text{CH}_3)_2\text{NCH}_2^+$, the (dimethylamino)methyl radical, $(\text{CH}_3)_2\text{NCH}_2^\bullet$, and the trimethylaminium radical cation, $(\text{CH}_3)_3\text{N}^{++}$, are predicted to belong to the point groups C_{2v} , C_s , and C_{3h} , respectively. Thus both cations are planar at nitrogen, while the neutral (dimethylamino)methyl radical has a pyramidal nitrogen center, $\gamma_N = 37.2^\circ$ (compared to $\gamma_N = 51.6^\circ$ for trimethylamine). In $(\text{CH}_3)_2\text{NCH}_2^\bullet$, the methylene group is also pyramidal, with $\gamma_C = 30.1^\circ$. As in the case of the parent compounds, the H₂C–N bonds increase in length in the same series: 1.285, 1.384, and 1.455 Å for $(\text{CH}_3)_2\text{NCH}_2^+$, $(\text{CH}_3)_2\text{NCH}_2^\bullet$, and $(\text{CH}_3)_3\text{N}$ (the H₃C–N bond in this case), respectively. It is apparent that methyl substitution at N has the opposite effect on the local geometry of the CH₂ group in type I or type II reactive intermediates, lengthening the former and shortening the latter. In the case of the aminium radical cation, $(\text{CH}_3)_3\text{N}^{++}$, the nitrogen center is (quasi)planar in each case, and the N–CH₃ bond, 1.448 Å (1.431 Å in $\text{H}_2\text{NCH}_3^{++}$), is also lengthened somewhat by the additional methyl substitution.

Energetic Considerations. The MP2/6-31+G* total energies of all species are listed in Table I. For the unmethylated species, G2 energies are provided as well. Although these quantities are not of primary interest in this study, simple differences in the total energies, taking into consideration zero-point energies in the case of the MP2 values, provide a rough measure of adiabatic ionization potentials, proton affinities, bond dissociation energies, the effects of methyl substitution on these quantities, and in the case of the tautomeric radical cations, $\text{H}_2\text{NCH}_3^{++}$ and $\text{H}_3\text{NCH}_2^{++}$, relative stabilities. All quantities, of course, are appropriate for the gas phase.

Adiabatic Ionization Potentials (IPs). Comparison of the G2 energies of H_2NCH_3 and $\text{H}_2\text{NCH}_3^{++}$ provides the IP of meth-

ylamine, 9.05 eV (expt¹¹ 8.97 ± 0.02 eV). The MP2/6-31+G* value is 8.58 eV for methylamine and 7.62 eV (expt¹¹ 7.82 ± 0.06 eV) for trimethylamine. Similarly, comparison of the G2 energies of $\text{H}_2\text{NCH}_2^\bullet$ and H_2NCH_2^+ provides the IP of aminomethyl free radical, 6.35 eV (expt¹⁸ 6.29 ± 0.03 eV). The MP2/6-31+G* value is 5.82 eV for aminomethyl radical and 5.08 eV for (dimethylamino)methyl radical (expt¹⁹ 5.9 ± 0.1 eV). The IPs of methylamine and the aminomethyl radical are both underestimated by the MP2/6-31+G* procedure by about 0.5 eV.

Proton Affinities (PAs). Comparison of the G2 energies of $\text{H}_2\text{NCH}_2^\bullet$ and the tautomers, $\text{H}_2\text{NCH}_3^{++}$ and $\text{H}_3\text{NCH}_2^{++}$, yields the gas-phase PAs of the carbon and nitrogen sites of the aminomethyl free radical, 8.37 and 8.41 eV (expt²⁰ 8.78 eV), respectively. The respective MP2/6-31+G* values are 8.44 and 8.58 eV. Thus, at both levels, the N-protonated form is predicted to be more stable in spite of the fact that, as noted above, the C–N bond is substantially shorter in the C-protonated isomer. The preferential solvation of the C-protonated form is discussed below. The N-protonated analog in the (dimethylamino)methyl system is not part of the present study. Comparison of the MP2/6-31+G* energies of the trimethylaminium radical cation, $(\text{CH}_3)_3\text{N}^{++}$, and the (dimethylamino)methyl radical, $(\text{CH}_3)_2\text{NCH}_2^\bullet$, yields an estimate for the energy of C protonation, 9.55 eV (expt²⁰ 9.41 eV). Thus, N,N-dimethylation is predicted to increase the PA of the C site of the aminomethyl radical by about 1.1 eV.

Bond Dissociation Energies (BDEs). Comparison of the G2 energies of H_2NCH_3 and $\text{H}_2\text{NCH}_2^\bullet$ yields the BDE at 0 K of the C–H bond of methylamine, 372 kJ mol⁻¹ (expt¹⁹ 393 ± 8 kJ mol⁻¹). The error in the G2 value is just outside the normal range of expected errors. A more accurate treatment (MP4/6-31+G** (2df) energies at MP2/6-31+G** geometries)²¹ afforded the value 392 kJ mol⁻¹. The MP2/6-31+G* value, taking $E(\text{H}) = -0.498 233$ hartree, is 348 kJ mol⁻¹ for methylamine and 350 kJ mol⁻¹ for trimethylamine (expt²⁰ 351 kJ mol⁻¹). Similarly, comparison of the G2 energies of $\text{H}_2\text{NCH}_3^{++}$ and H_2NCH_2^+ provides the equivalent BDE of the methylaminium radical cation, 107 kJ mol⁻¹ (expt²⁰ 121 kJ mol⁻¹). The N–H BDE of $\text{H}_3\text{NCH}_2^{++}$ may

(18) Dyke, J. M.; Lee, E. P. F.; Niavarani, M. H. *Z. Int. J. Mass. Spectrom. Ion Processes* 1989, 94, 221.

(19) Griller, D.; Lossing, F. P. *J. Am. Chem. Soc.* 1981, 103, 1586.

(20) Calculated based on the heats of formation in ref 11.

(21) Leroy, G.; Sana, M.; Wilante, C. *J. Mol. Struct.* 1991, 228, 37.

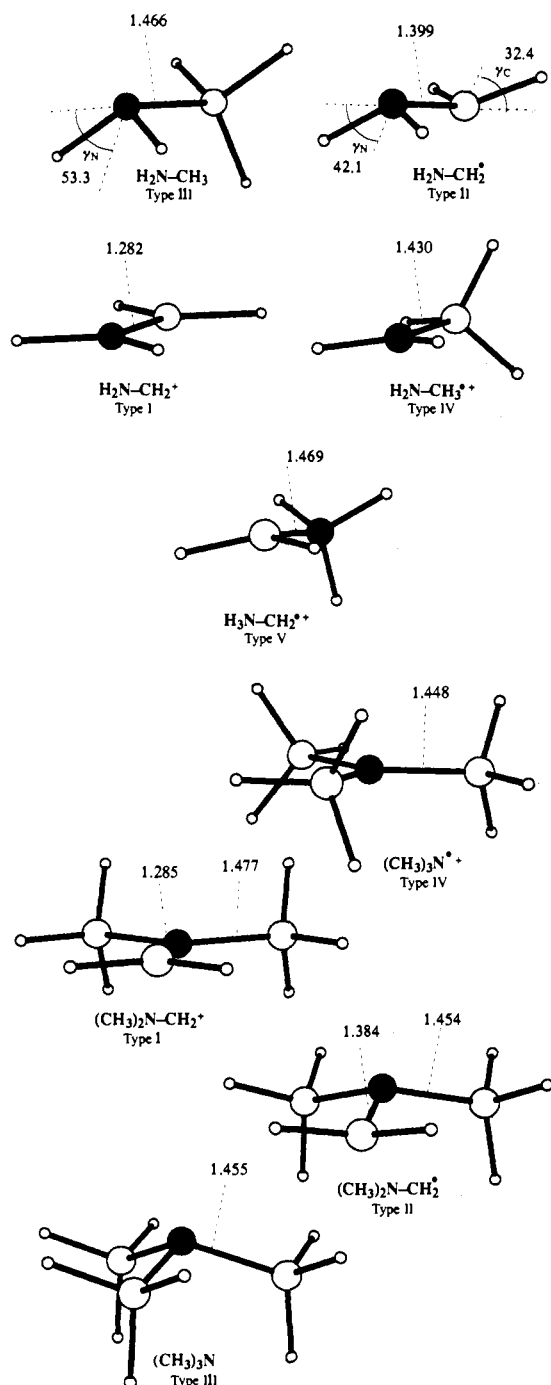


Figure 1. MP2/6-31+G* optimized structures. The filled balls stand for nitrogen atoms and the open ones for carbon (large) and hydrogen (small). Bond lengths are in angstroms and angles in degrees.

be similarly derived (111 kJ mol^{-1} ; G2) and reflects the 4 kJ mol^{-1} difference in stabilities of the tautomeric radical cations at 0 K. The MP2/6-31+G* values are 68 and 81 kJ mol^{-1} , respectively. The C-H BDE of the trimethylaminium radical cation is 104 kJ mol^{-1} (MP2/6-31+G*, expt²⁰ 121 kJ mol^{-1}). Comparison of the MP2/6-31+G* values for $\text{H}_2\text{NCH}_3^{+\bullet}$ and $(\text{CH}_3)_3\text{N}^{+\bullet}$ suggests that stabilization of the aminium radical cation center by the two methyl groups on the nitrogen atom is about 36 kJ mol^{-1} , substantially less than predicted for proton loss from the same system, 106 kJ mol^{-1} (= 1.1 eV, previous section).

Infrared Frequencies and Intensities. Calculated harmonic frequencies and infrared intensities (HF/6-31G*) for all species have been submitted as supplementary data. We discuss here only the main features predicted for the IR spectra of the reactive intermediates in the hope that the discussion may aid in their

spectroscopic identification. In the following discussion, the frequencies cited have been reduced in magnitude by a factor of 0.89.

As expected in the case of the charged species, very strong IR absorptions are calculated to be associated with normal modes which involve motion of nuclei bearing large formal charges. Thus, in the case of the iminium cation, H_2NCH_2^+ , the symmetric and antisymmetric N-H stretching vibrations are predicted to occur at 3316 and 3411 cm^{-1} and have intensities of 193.4 and 220.5 km mol^{-1} , respectively. The C-N stretch is predicted to have an intensity of 129.6 km mol^{-1} and to occur at 1721 cm^{-1} . This mode is strongly mixed with the NH_2 scissoring motion. The computed position agrees moderately well with that deduced from photoionization spectroscopy (1810 cm^{-1}) of the neutral aminomethyl radical.¹⁸ The most intense absorption of the iminium cation, 314.0 km mol^{-1} , is associated with the wagging motion (out-of-plane bending) of the NH_2 group at 909 cm^{-1} . Upon methylation at N, i.e., $(\text{CH}_3)_2\text{NCH}_2^+$, the H₂C-N stretch, at 1730 cm^{-1} , is weakened, 79.8 km mol^{-1} . This mode is mixed with the CH_2 scissoring motion. The other principal absorptions are predicted as follows (wave number (intensity)): 1482 (66.4), CH_2 scissor and methyl deformation; 1448 (43.0), methyl deformation; 1302 (23.3), CH_2 rock and asymmetric N- CH_3 stretch; 1129 (22.8), CH_2 wag; 968 (33.6) CH_2 rock and asymmetric N- CH_3 stretch.

The methylaminium radical cation (type IV), $\text{H}_2\text{NCH}_3^{+\bullet}$, has many features in common with the iminium cation discussed above. The N-H stretches are predicted to occur at 3262 and 3368 cm^{-1} , with intensities of 113.4 and 216.9 km mol^{-1} , respectively. The NH_2 scissor, which dominates the mode that was mixed with the C-N stretching motion, is at lower frequency, 1569 cm^{-1} , and is less intense, 51.7 km mol^{-1} . The out-of-plane NH_2 deformation (NH_2 wag) occurs at 678 cm^{-1} with intensity of 165.4 km mol^{-1} . The predicted IR spectrum of the trimethylaminium radical cation, $(\text{CH}_3)_3\text{N}^{+\bullet}$, is (wave number (intensity)): 1443 (49.6), 1432 (57.8), methyl deformations; 1399 (19.9), methyl umbrella; 970 (34.4), methyl rock mixed with C-N stretch.

The type V radical cation, $\text{H}_3\text{NCH}_2^{+\bullet}$, in which the nitrogen atom bears the formal positive charge is predicted to have a number of very strong absorptions, most of which are associated with stretches and angle bending motions of the NH_3^+ group. The predicted spectrum is as follows ((wave number (intensity)): 3297 (174.3), 3270 (163.5), 3191 (67.7), N-H stretches; 1614 (126.8), NH_3 deformations; 1516 (154.9), NH_3 umbrella; 473 (79.4), CH_2 wag.

The neutral aminomethyl radical, $\text{H}_2\text{NCH}_2^\bullet$, has moderately strong absorptions in the CH stretching region, 2941 and 3033 cm^{-1} , with intensities of 29.2 and 36.9 km mol^{-1} , respectively, and in the region of the C-N stretch, 1122 cm^{-1} (31.9 km mol^{-1}). However, the NH_2 scissor at 1630 cm^{-1} has higher intensity (45.5 km mol^{-1}), as do both combinations of the NH_2 and CH_2 wags at 694 and 797 cm^{-1} , with intensities of 267.7 and 66.1 km mol^{-1} , respectively. In the (dimethylamino)methyl radical, $(\text{CH}_3)_2\text{NCH}_2^\bullet$, the strongest absorptions are predicted to arise from two methyl C-H stretching combinations at 2812 and 2892 cm^{-1} , with intensities of 126.4 and 83.4 km mol^{-1} , respectively. Three other absorptions of moderate strength are predicted ((wave number (intensity)): 1329 (58.1), N- CH_2 stretch; 1294 (35.1), CH_2 rock mixed with N- CH_3 stretch; 1075 (41.8), N- CH_3 stretch mixed with methyl rocking.

4. Thermochemical Data and Discussion

Gas-Phase Thermodynamic Functions. The gas-phase thermodynamic functions C_p° , S° , and $H^\circ - H^\circ_0$ were calculated from the ab initio vibrational frequencies using the standard statistical methods. In standard statistical methods, hindered internal rotations are treated as vibrational motions rather than as free rotors. This approximation may entail some error in the calculated thermodynamic functions, C_p° , S° , and $H^\circ - H^\circ_0$, which could be avoided in a more detailed treatment.²² In the present work we have neglected the uncertainties in C_p° , S° , and $H^\circ - H^\circ_0$

Table II. Thermochemical Data at 298.15 K

species	type	$\Delta_f H^\circ(\text{g})^a$ (kJ mol ⁻¹)	$S^\circ(\text{g})^b$ (J K ⁻¹ mol ⁻¹)	$\Delta_f G^\circ(\text{g})^c$ (kJ mol ⁻¹)	$\Delta_f G^\circ(\text{aq})^c$ (kJ mol ⁻¹)
H ₂ NCH ₂ ⁺	I	745 ^d 760 ^e	239 (2) 224 ^e	782	
H ₂ NCH ₂ [*]	II	150.6 ^f 148 ^e	250 (1) 243 ^e	183 ± 8	172 ± 10
HNCH ₃ [*]	VI	182	236 (3)	220 ± 8	210 ± 12
H ₂ NCH ₃ ^{**}	IV	842 869 ^e	243 (6) 260 ^e	897 ± 2	561 ± 15
H ₃ NCH ₂ ^{**}	V	≤841 865 ^e	253 ^e		
H ₂ NCH ₃	III	-23.0 ^e	243.4 ^e 243 (3) 240 ^e	32.2 ± 2 ^f	20.8 ± 3 ^g
H ₃ NCH ₃ ⁺	VII	611	244 (9)	685 ± 12	379 ± 5 ^h
CH ₃ NHCH ₂ ⁺	I	695 ^d	275 (3)	762	
CH ₃ NHCH ₂ [*]	II	126	280 (3)	191 ± 8	181 ± 10
(CH ₃) ₂ N [*]	VI	145	260 (18)	216 ± 8	210 ± 15
(CH ₃) ₂ NH ^{**}	IV	776	273 (18)	863 ± 8	555 ± 18
(CH ₃) ₂ NH	III	-18.5 ^e	273.1 ^e 273 (9)	68.5 ± 2	58.3 ± 2
(CH ₃) ₂ NH ₂ ⁺	VII	588	277 (18)	695 ± 12	416 ± 5 ^h
(CH ₃) ₂ NCH ₂ ⁺	I	661 ^d	299 (18) 293 ^e	761	
(CH ₃) ₂ NCH ₂ [*]	II	109	310 (9) 307 ^e	206 ± 10	200 ± 12
(CH ₃) ₃ N ^{**}	IV	731	294 (162) 327 ^e	852 ± 7	573 ± 15
(CH ₃) ₃ N	III	-24.3 ^e -23.7	287.1 ^e 294 (81) 299 ^e	99.1 ^e 97.4 ± 2	91.5 ± 3
(CH ₃) ₃ NH ⁺	VII	564	304 (81)	704 ± 12	456 ± 5 ^h
H ₂ NCHCH ₃ ⁺	I	657 ^d	275 (3)	724	
H ₂ NCHCH ₃ [*]	II	109	280 (3)	174 ± 8	163 ± 10
H ₂ NCH ₂ CH ₃ ^{**}	IV	807	283 (6)	891 ± 4	566 ± 15
H ₂ NCH ₂ CH ₃	III	-47.5 -47.2 ^e	283 (3)	36.6 ± 2	25.5 ± 3
H ₃ NCH ₂ CH ₃ ⁺	VII	574	283 (9)	678 ± 12	383 ± 5

^a From ref 11 unless otherwise noted. ^b Unless otherwise noted, from this study calculated as described in the text. Symmetry numbers used are indicated in parentheses. ^c Unless otherwise noted, from this study calculated as described in the text. ^d Original value from ref 41 preferred by Lias et al.¹¹ ^e From this study. ^f $\Delta_f H^\circ(\text{g})$ values were based on the G2 energies and $S^\circ(\text{g})$ on HF/6-31G* frequencies as described in the text. ^g From ref 24. ^h From ref 16.

which may be introduced by the treatment of internal rotations as vibrations. In most cases these are expected to be less than the errors arising from calculated vibrational frequencies. Values of $\Delta_f H^\circ_0$ were derived directly from the G2 energies according to $\Delta_f H^\circ_0 = E(\text{G2}) - \sum E(\text{G2 elements})$ for H₂NCH₂⁺, H₂NCH₂^{*}, H₂NCH₃, H₂NCH₃^{**}, and H₃NCH₂^{**}. Using calculated $H^\circ - H^\circ_0$ and the experimental values of heats of formation at 298 K as reference values, $\Delta_f H^\circ_T$ values were calculated for all of the molecules studied in this work at $T = 0, 100, 200,$ and 298 K. The corresponding $\Delta_f G^\circ_T$ were also evaluated with the calculated S° and $\Delta_f H^\circ_T$. The data are collected in Table S-III of the supplementary material.

Gas-phase values of S°_{298} , $\Delta_f H^\circ_{298}$, and $\Delta_f G^\circ_{298}$ obtained from the G2 energies for methylamine and the radical and iminium species related to it are listed in Table II. Also tabulated are experimental heats of formation, taken from the literature. In regard to the experimental values of $\Delta_f H^\circ_{298}$, it may be noted that the greatest weight has been given to the recent compilation of Lias et al.,¹¹ which contains extensive data for both neutrals and ions. In fact, unless otherwise noted, all data used in the thermochemical calculations of the next section are based on heats of formation from that source.

For the determination of thermodynamic properties, the residual errors in the G2 energy are too high in many cases, and isodesmic and isogyric reactions should be used to provide the more accurate values of $\Delta_f H^\circ$ required. This is also true in the cases of (CH₃)₂NCH₂⁺, (CH₃)₂NCH₂^{*}, (CH₃)₃N, and (CH₃)₃N^{**}, but isodesmic reactions were not carried out extensively here. However, one of the objectives of the ab initio calculations in this study was to gain information on the geometries and thermodynamic

Table III. Free Energies of Solution^a

neutrals	$-\Delta G^\circ(\text{soln})^b$ (kJ mol ⁻¹)	ions	$-\Delta G^\circ(\text{soln})^c$ (kJ mol ⁻¹)
CH ₃ NH ₂	11.4	CH ₃ NH ₃ ⁺	306
CH ₃ CH ₂ NH ₂	11.1	CH ₃ CH ₂ NH ₃ ⁺	295
CH ₃ CH ₂ CH ₂ NH ₂	10.7		
(CH ₃) ₂ NH	10.2	(CH ₃) ₂ NH ₂ ⁺	278
(CH ₃) ₃ N	5.9	(CH ₃) ₃ NH ⁺	249

^a Standard states are 1 bar for gases and 1 M for solutes in aqueous solution. ^b Based on data in ref 27. ^c Absolute free energies of solution based on^{22,43} $\Delta_f G^\circ(\text{aq})(\text{H}^+) = 419$ kJ mol⁻¹ and $\Delta G^\circ(\text{soln})(\text{H}^+) = -1098$ kJ mol⁻¹ and calculated from data in refs 16 and 26.

properties of the amine-derived reactive intermediates, and one may note that the heats of formation derived from the G2 results for the species of the methylamine system were all within ±15 kJ mol⁻¹ of those recommended in the compilation of Lias et al.¹¹ (see Table II). This is a measure of the absolute confidence level of G2 theory and is comparable to that observed in previous G2 computations.^{13,23} In particular, it is worth noting that the value of 148 kJ mol⁻¹ for the heat of formation of H₂NCH₂^{*} is close to the experimental result of 150.6 kJ mol⁻¹ reported by Griller et al.²⁴ This G2 result and the theoretical study of Leroy et al.²¹ therefore support the preference for the higher experimental values relative to the older result²⁵ of 131 kJ mol⁻¹. The entropies calculated based on the scaled HF/6-31G* frequencies for the methylamine system agree quite well with those obtained by the additivity relationships or, where available, those given by Wagman et al.¹⁶

Free Energies of Solution of Radicals. Table III contains free energies of solution, viz., $\Delta_f G^\circ_{298}$, for



for several amines and some related compounds taken from the literature.^{16,26,27} For the neutral compounds it may be noted that the overall change in $\Delta G^\circ(\text{soln})$ over the range of different structures is from 6 to 11 kJ mol⁻¹. This is much less than the overall free energy changes usually encountered in reactions 1–6 (see below). Therefore, when neutral species similar to those in Table III are involved, errors introduced by the estimation of the solution energy contributions are fairly minor. However, this will not be the case when ionic species are involved. As the data in Table III show, the solution energies, and hence the potential magnitudes of error in their estimation, are a factor of 10 larger. Thus we begin this section by first discussing neutral species.

Comparison of the values for methyl-, ethyl-, and *n*-propylamine in Table III indicates that $\Delta G^\circ(\text{soln})$ is not sensitive to the size of the aliphatic side group, provided the changes are held within reasonable limits. The decrease in magnitude in going from primary to secondary to tertiary amine seen in Table III confirms that it is determined primarily by the substitution pattern around the N atom. Following Schwarz and Dodson's²⁸ approach to the alcohol species, it is helpful to treat the amino group interaction with water in terms of hydrogen bonding. The solution free energies can then be separated into hydrogen-bonding (HB) and non-hydrogen-bonding (NHB) components. The NHB component ($\Delta G^\circ(\text{NHB})$) will be an endoergic term representing the sum of the energies for cavity formation and van der Waals interactions.²⁹ From the values for $\Delta G^\circ(\text{soln})$ of ethane and other similar sized nonpolar molecules, this is assumed to be 15.5 kJ mol⁻¹.²⁸ From the decreases in the magnitude of $\Delta G^\circ(\text{soln})$ in going from me-

(23) Yu, D.; Rauk, A.; Armstrong, D. A. *J. Phys. Chem.* 1992, 96, 6031.(24) Burke, T. J.; Castelano, A. L.; Griller, D.; Lossing, F. P. *J. Am. Chem. Soc.* 1983, 105, 4701.(25) Grela, M. A.; Colussi, A. J. *J. Phys. Chem.* 1984, 88, 5995.(26) Perrin, D. D. *Dissociation Constants of Organic Bases in Aqueous Solution*; IUPAC; Butterworths: London, 1965.(27) Cabani, S.; Gianni, P.; Mollica, V.; Lepori, L. *J. Solution Chem.* 1981, 10, 563.(28) Schwarz, H. A.; Dodson, R. W. *J. Phys. Chem.* 1984, 88, 3643.(29) Taft, R. W.; Wolf, J. F.; Beauchamp, J. L.; Scorrano, G.; Arnett, E. M. *J. Am. Chem. Soc.* 1978, 100, 1240.

Table IV. Reduction Potentials and Radical Ionization Energy^a

amine	$E^{\circ}_{(2)}$ (V)	$-\Delta G^{\circ}(\text{soln of R})^b$ (kJ mol ⁻¹)	$-\Delta G^{\circ}_{(3)}$ (kJ mol ⁻¹)	$E^{\circ}_{(6)}$ (V)
H ₂ NCH ₃	1.56	336	30	1.25
H ₂ NCH ₂ CH ₃	1.42	325	16	1.25
HN(CH ₃) ₂	1.27	308	45	0.80
(CH ₃) ₃ N	1.13	279	46	0.65

^a Calculated as described in section 4. Values in italics were calculated assuming $\Delta G^{\circ}(\text{soln of R}^1\text{R}^2\text{NCR}^3\text{H}_2^{+\bullet}) = \Delta G^{\circ}(\text{soln of R}^1\text{R}^2\text{NHCR}^3\text{H}_2^{+\bullet}) - 30 \text{ kJ mol}^{-1}$. ^b R = R¹R²NCR³H₂^{+\bullet}.

thylamine to ethylamine to *n*-propylamine, there is evidently an increase of 0.5 kJ mol⁻¹ in $\Delta G^{\circ}(\text{NHB})$ per added CH₂ group. The values of the HB components ($\Delta G^{\circ}(\text{HB})$) can then be calculated from $\Delta G^{\circ}(\text{HB}) = \Delta G^{\circ}(\text{soln}) - \Delta G^{\circ}(\text{NHB})$, where the latter term is adjusted for n_{Me} , the total number of methyl and/or methylene groups. The value for trimethylamine (-22.4 kJ mol⁻¹) represents the N:→H-OH lone pair contribution, $\Delta G^{\circ}(\text{HBNLP})$, which will also apply with methylamine and dimethylamine. Using the results for the five amines in Table III, the value of the N-H...:OH₂ contribution ($\Delta G^{\circ}(\text{HBNH})$) is then found to be -3.8 kJ mol⁻¹ for one N-H...:OH₂ bond and -4.6 kJ mol⁻¹ when two N-H...:OH₂ bonds are involved. These observations may be compared with the case for water, where a single average hydrogen-bond energy of -9.2 kJ mol⁻¹ has been used to explain the data.²⁸ That there are two different kinds of hydrogen bond involved in the amine-water interactions is obvious. The differences between their magnitudes and between each of these and the bonds in the ROH system are easily rationalized in terms of the relative basicities of N and O lone pairs and the relative acidities of the N-H and O-H bonds.

On the basis of the above analysis, the values of $\Delta G^{\circ}(\text{soln})$ for the neutral radicals can be calculated with

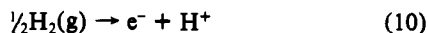
$$\Delta G^{\circ}(\text{soln})/\text{kJ mol}^{-1} = 15.5 + 0.5(n_{\text{Me}}) - 22.4 - q(n_{\text{N-H:OH}}) \quad (8)$$

where $q = 4.6$ and 3.8 for $(n_{\text{N-H:OH}}) = 2$ and 1 , respectively. The values found for the α -amino radicals, species II, are then the same as those for the parent amines, species III. Reference to Figure 1 and Table I provides an alternative justification for this on structural grounds. For both methylamine and trimethylamine, the radical and the amine have similar geometry and only minor differences in charge distribution. The only significant difference in each case is the loss of the relatively nonpolar C-H bond, and this would also be true for the other two amine systems in Table II. Since the net effect is a negligibly small change in the sizes of the aliphatic side groups, in the light of the data in Table III it is evident that any difference in $\Delta G^{\circ}(\text{soln})$ of R¹R²NCR³H^{\bullet} and that of the corresponding R¹R²NCR³H₂ will be <2 kJ mol⁻¹. The values of $\Delta_r G^{\circ}(\text{aq})$ for the type II radicals in Table II were calculated on that basis.

Radical Reduction Potentials. The value of the reduction potential, $E^{\circ}_{(2)}$, for reaction 2 (R¹R²NCR³H^{\bullet} + e⁻ + H⁺ → R¹R²NCR³H₂) is defined by $E^{\circ}_{(2)} = -\Delta G^{\circ}_{(9)}/F$, where F is the Faraday constant and $\Delta G^{\circ}_{(9)}$ is the free energy change of the complete reaction 9:³⁰



This reaction is obtained from eq 2 by addition of the standard half-reaction:



Hence, the values of $E^{\circ}_{(2)}$ can be calculated from the $\Delta_r G^{\circ}(\text{aq})$ data for the R¹R²NCR³H^{\bullet} and R¹R²NCR³H₂ species in Table II. Unless otherwise stated, similar procedures were used in calculating the reduction potentials for the other half-reactions considered here. The results are presented in Table IV.

(30) In chemical equations (g) denotes species in the gas phase with standard state 1 bar. The absence of any designation indicates aqueous solution, standard state 1 mol dm⁻³.

Table II also contains the gas-phase free energies of formation of the N-centered R¹R²N^{\bullet} radicals for the cases R¹ = H, R² = CH₃ and R¹ = R² = CH₃, which were not part of the computational study. These radicals may undergo a reduction half-reaction similar to eq 2, namely, reaction 11 with reduction potential $E^{\circ}_{(11)}$:



Since they have been postulated to occur in aqueous systems,³¹⁻³⁴ it is of interest to find the values of $\Delta G^{\circ}(\text{aq})$ for them and obtain estimates of these potentials. The solution energies calculated with the equation derived above (eq 8) are -10.7 and -6.4 kJ mol⁻¹, respectively. The values of $\Delta G^{\circ}(\text{aq})$ have been given in Table II, and $E^{\circ}_{(11)}$ was found to be 1.96 V for CH₃NH^{\bullet} and 1.57 V for CH₃NCH₃^{\bullet}. Hence, these radicals are stronger oxidants than their aminoalkyl counterparts.

Free Energy of Solution of Aminium Ions and $E^{\circ}_{(6)}$. Attention is now directed to reaction 3. Values of radical pK 's have been reported for the radicals of several of the simple amines,³¹⁻³⁴ but the most reliable value appears to be that reported for trimethylamine.⁷ Here the identities of the radicals present in aqueous solution above and below the pK value have been established by ESR techniques and chemical reactivity, and the value of $\Delta G^{\circ}_{(-3)}$ has been shown by Das and von Sonntag⁷ under conditions of careful buffering to be 45.6 kJ mol⁻¹ ($pK_{(-3)} = 8.0$). Since eq 6 is equivalent to eq 2 minus eq 3, the value of $E^{\circ}_{(6)}$ can be found from $E_{(6)} = E^{\circ}_{(2)} - \Delta G^{\circ}_{(3)}/F$. The value of $E^{\circ}_{(6)}$ obtained by this method is listed in Table IV.

The magnitude of $\Delta G^{\circ}_{(3)}$ for trimethylamine provides another important thermochemical result. From it and the values of $\Delta_r G^{\circ}(\text{aq})$ of H⁺ and (CH₃)₃NCH₃^{\bullet} (i.e., R¹R²NCR³H^{\bullet} for this system) in Table II, one finds $\Delta_r G^{\circ}(\text{aq})$ of (CH₃)₃N^{+\bullet} equal to 573 kJ mol⁻¹. Using that value in conjunction with $\Delta_r G^{\circ}(\text{g})$ for this species from Table II leads to a value of $\Delta G^{\circ}(\text{soln})$ for (CH₃)₃N^{+\bullet} of -279 kJ mol⁻¹, which is 30 kJ mol⁻¹ larger in magnitude than the value of -249 kJ mol⁻¹ for (CH₃)₃NH⁺ (see Table III). From this difference it appears that the planar geometry of the aminium radical species (Figure 1) permits enhanced solvation by allowing water molecules on either side of the N^{+\bullet} center to approach much closer to it than is the case with the tetrahedral ammonium species R¹R²NHCR³H₂⁺. One can anticipate that the free energies of solution R¹R²NCR³H₂^{+\bullet} species will in general be larger than those for the corresponding R¹R²NHCR³H₂⁺ species, the values of which are listed in Table III. A similar conclusion was drawn earlier by Pearson³⁵ for NH₃^{+\bullet}, on the basis of a somewhat different line of reasoning. The fact that the radical pK 's may be larger than 8 for methylamine and ethylamine^{31,32} means that the excess solution energies for these cases may be even greater than 30 kJ mol⁻¹. However, in view of the problems encountered experimentally with trimethylamine,⁷ it is necessary to establish the identities of the radicals above and below the pK 's for those systems and to ensure that true equilibrium pK 's are obtained. Therefore for the present purposes, estimates of $\Delta G^{\circ}(\text{soln})$ of R¹R²NCR³H₂^{+\bullet} were made for methylamine, dimethylamine, and ethylamine on the assumption that the 30 kJ mol⁻¹ increase in solution free energy of (CH₃)₃N^{+\bullet} over that of (CH₃)₃NH⁺ would apply for all of the R¹R²NCR³H₂^{+\bullet} species. Values of $\Delta G^{\circ}_{(3)}$ were then found from $\Delta_r G^{\circ}(\text{aq})$ for those species, R¹R²NCR³H₂^{+\bullet}, and H⁺. These free energy changes have been presented in Table IV and were used to obtain the estimates of $E^{\circ}_{(6)}$ given there for the amines other than trimethylamine.

Applications to Redox Systems. The values of $E^{\circ}_{(2)}$ are the most reliable in Table IV with their uncertainty ~0.1 V determined by the errors in $\Delta_r H^{\circ}_{298}$ of the radicals. They are seen to reflect the trend in C-H bond dissociation energies of the amines,

(31) Simic, M.; Neta, P.; Hayon, E. *Int. J. Radiat. Phys. Chem.* 1971, 3, 309.

(32) Getoff, N.; Schwörer, F. *Int. J. Radiat. Phys. Chem.* 1971, 3, 429.

(33) Neta, P.; Fessenden, R. W. *J. Phys. Chem.* 1971, 75, 738.

(34) Fessenden, R. W.; Neta, P. *J. Phys. Chem.* 1972, 76, 2857.

(35) Pearson, R. G. *J. Am. Chem. Soc.* 1986, 108, 6109.

which increase in the same order. This feature has already been pointed out for nonaqueous systems by Griller et al.¹⁰ The values of $E^\circ_{(6)}$ are of special importance for the interpretation of electron transfer, and it is regrettable that the pK_R of the $R^1R^2NCR^3H_2^{++}$ radical, which is required for the calculation of this potential, is accurately known only for methylamine. However, the values for the other amines in Table IV are in line with the strong trend of increasing resistance to oxidation, which has been observed experimentally as one proceeds from primary to secondary to tertiary amines.⁶ The values of $E^\circ_{(6)}$ for trimethylamine and dimethylamine in Table IV are both significantly lower than the anodic potentials of 1.27 and 1.00 V, respectively, determined for them at pH 12 by cyclic voltammetry.⁶ This is presumably due to the irreversible nature of the electrode process. The present value of $E^\circ = 0.65$ V for reaction 12:



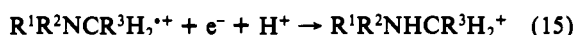
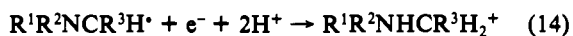
may be compared with 0.71 V estimated by Pearson using a thermochemical cycle with solution free energies of ionic species.³⁵ It also agrees well with experimental results for tertiary amines, for which reversible electrode kinetics was observed. One example would be 1-azabicyclo[3.3.3]undecane, for which $E^\circ_{(6)}$ is 0.62 V. It is noteworthy that the cation in this case is able to relax to the preferred planar configuration, which is expected for unconstrained $R^1R^2NCR^3H_2^{++}$ species (Figure 1). Also, the structure of this cation apparently precludes facile deprotonation, which is one cause of irreversibility.⁶

The fact that $E^\circ_{(6)}$ values for tertiary amines are substantially smaller than their anodic peak potentials is well established from the observation that measurable rates of oxidation can be obtained in alkaline aqueous solution with ferricyanide,^{36,37} for which $E^\circ(Fe(III)/Fe(II)) = 0.36$ V.³⁷ Here, as in other thermal oxidations of amines, the driving force for reaction arises primarily from the deprotonation reaction (-3). Based on the values of $-\Delta G^\circ_{(3)}$ in Table IV, the values of $\Delta G^\circ_{(-3)}$ at pH 12 would be -39, -53, and -23 kJ mol⁻¹ for methylamine, ethylamine, and di- and trimethylamine, respectively. Deprotonation transforms the aminium radical into $R^1R^2NCR^3H^\cdot$, the α -aminoalkyl radical. With typical oxidants such as ClO_2 or $Fe(CN)_6^{3-}$, a second molecule is rapidly reduced by this species.⁶

It is evident that, as the pH becomes more acidic, first the amines ($pK_{(13)} \approx 10$)²⁶ and then the radicals ($pK_{(-3)} \approx 8$) will become protonated.



Thus one has reactions 2, 14, and 15



dominating in the pH regions: $pH > pK_{(13)}$, $pK_{(13)} > pH > pK_{(-3)}$, and $pK_{(-3)} > pH$, respectively. Following the conventions in ref 38, the expression for $E_{h(\text{radical/amine})}$, the potential for the half-cell with total radical and amine concentrations of $[R_T]$ and $[A_m]$, respectively, is

$$E_{h(\text{radical/amine})} =$$

$$E^\circ_{(2)} + \frac{RT}{F} \ln \frac{a_H [R_T]}{[A_m]} + \frac{RT}{F} \ln \frac{\frac{1}{\gamma_A} + \frac{a_H}{\gamma_{AH} K_{13}}}{\frac{1}{\gamma_R} + \frac{a_H}{\gamma_R K_{(-3)}}} \quad (16)$$

Here a_H is the hydrogen ion activity, γ_R , γ_{R^\cdot} , γ_A , and γ_{AH} are the activity coefficients of the aminium radical cation, the α -amino radical, the amine, and the protonated amine, respectively, and

(36) Smith, J. R. L.; Mead, L. A. V. *J. Chem. Soc., Perkin Trans. 2* 1973, 206.

(37) Hull, L. A.; Davis, G. T.; Rosenblatt, D. H. *J. Am. Chem. Soc.* 1969, 91, 6247.

(38) Wardman, P. *J. Phys. Chem. Ref. Data* 1989, 18, 1637.

the other symbols have already been defined. As an example, for trimethylamine with $[R_T] = [A_m]$, $E_{h(\text{radical/amine})}$ has values of 1.13, 0.73, 0.55, and 0.48 V at pH's of 0, 5, 9, and 11, respectively. It may be noted that $E_{h(\text{radical/amine})}$ falls below $E^\circ_{(6)}$ at high pH, because of the deprotonation of the radical.

Another feature of the pH dependence of $E_{h(\text{radical/amine})}$ is that, even for the tertiary amine, $E_{h(\text{radical/amine})}$ rises above 1.0 V, and relatively strong oxidants are required to oxidize amines at low pH. One oxidant frequently used, particularly in radiation chemistry, is the OH^\cdot radical with $E^\circ(OH^\cdot/OH^-) = 1.80$ V.^{28,39} This redox potential is large enough that radicals may be produced by H atom abstraction from either the nitrogen center or a carbon center of a protonated amine. Thus in acid solutions of trimethylamine, Das and von Sonntag⁷ found evidence for $(CH_3)_2NHCH_2^{++}$, as well as the species already discussed above. At equilibrium this species was about 10 000-fold less abundant than $(CH_3)_3N^{++}$. Lias et al.¹¹ did not list any data for this species, and it was not included in our calculations. However, in this study the methylamine analog, $NH_3CH_2^{++}$, was investigated in a G2 level calculation. As shown by the $\Delta_r H^\circ_{298}$ values in Table II, in the gas phase this species turns out to be slightly more stable than the aminium radical counterpart $NH_2CH_3^{++}$, a result which is also supported by the available experimental data. One might anticipate a similar stability for $(CH_3)_2NHCH_2^{++}$ were it not for the fact that in section 3 methyl substitution was shown to enhance the stability of the type IV species. The smaller stability in solution may additionally be rationalized on the premise that the solution free energy of the species with tetrahedral nitrogen will be less than that of the planar aminium ion (see above).

Also of interest are CH_3NH^\cdot and $CH_3NCH_3^\cdot$, which may be produced by H atom abstraction from the N centers of methylamine and dimethylamine. As shown by the $\Delta_r G^\circ(\text{aq})$ values in Table II, these species are less stable than the α -aminoalkyl radicals. Hence, these also would not be present in significant concentrations at equilibrium. In support of this, ESR experiments showed no evidence for $CH_3NCH_3^\cdot$ in irradiated aqueous dimethylamine solutions, but did show a spectrum attributable to $CH_3NHCH_3^{++}$ at pH 1-5.³⁴ The lines for that species faded out near pH 6, which is expected if the pK is 8, as calculated from our $-\Delta G^\circ_{(3)}$ in Table IV. When produced from $(CH_3)_2NCl$ photolysis, $CH_3NCH_3^\cdot$ was protonated on the time scale of the ESR experiment at pHs up to 5, and only $CH_3NHCH_3^{++}$ was observed. No lines were resolvable at pH 7, but at pH 8 $CH_3NCH_3^\cdot$ was seen. At that pH, with a protonation rate constant of 10^{10} dm³ mol⁻¹ s⁻¹, the relaxation time for protonation would be $>10^{-3}$ s. Since protonation to $CH_3NHCH_3^{++}$



followed by deprotonation to $CH_3NHCH_2^\cdot$ in reaction -3 is probably the only facile way for the N- and C-centered radicals to achieve equilibration, this observation does not preclude the lower stability of $CH_3NCH_3^\cdot$ indicated by the data in Table II. In this regard one may note that Das and von Sonntag⁷ used very high concentrations of buffer in order to achieve equilibrium between the $(CH_3)_3N^{++}$ and $(CH_3)_2NCH_2^\cdot$ trimethylamine species. It would therefore be of interest to repeat the earlier pulse radiolysis experiments with other amines at larger buffer concentrations. One might then be able to properly identify $pK_{(-3)}$ for those amines.

Finally, attention is directed to reaction 5 ($R^1R^2NCR^3H^+ + e^- + H^+ \rightarrow R^1R^2NCR^3H_2^{++}$). Since $R^1R^2NCR^3H^+$ and $R^1R^2NCR^3H_2^{++}$ have the same charge and again differ in only one H atom, the approximation is made that their solution free energies are equal. Reference to Figure 1 confirms that the overall geometries of these species are similar for the cases of methylamine and trimethylamine, but the charge distributions are not identical (Table I). The approximation of equal solution energies will not therefore be as good as it was in the case of reaction 2 above (i.e., errors of ± 15 kJ mol⁻¹). However, at this time there is no method

(39) Klänning, U. K.; Sehested, K.; Holcman, J. *J. Phys. Chem.* 1985, 89, 760.

for correcting for the change in charge distribution, and the present approach represents the most accurate method of obtaining an estimate of $E^{\circ}_{(5)}$. The resulting values of $E^{\circ}_{(5)}$ were -1.19, -1.73, -1.05, and -0.94 V for methylamine, ethylamine, dimethylamine, and trimethylamine, respectively. Likewise, utilizing the values of $\Delta G^{\circ}_{(3)}$ derived above, one can estimate that $E^{\circ}_{(1)}$ has values of about -1.5, -1.9, -1.5, and -1.4 V for the same amines, respectively. The large negative values of $E^{\circ}_{(1)}$ confirm the strong reductive power of these $R^1R^2NCR^3H^{\bullet}$ radicals. Previous estimates of $E^{\circ}_{(1)}$ in aqueous solution have been in the region of -1.0 V.⁴⁰ Equilibrium measurements of these quantities in water will be very difficult because of the transitory nature of both the radicals and the iminium products. Thus, this is a case where theoretical investigations of the solution free energies of the iminium species would be of considerable interest, since they have the potential to reduce the uncertainties in the calculation of $E^{\circ}_{(1)}$.

5. Summary

In the present work, thermochemical functions for aminoalkyl and alkylaminium free radicals and related species were derived by combining results from high-level ab initio calculations with

- (40) (a) Adrieun, P. A.; Saveant, J. M. *Bull. Soc. Chim. Fr.* **1968**, 4671. (b) Monserrat, K.; Foreman, T. K.; Grätzel, M.; Whitten, D. G. *J. Am. Chem. Soc.* **1981**, *103*, 6667. (c) Hiller, K. O.; Asmus, K. D. *J. Phys. Chem.* **1983**, *87*, 3682.
 (41) Lossing, F. P.; Lam, Y. T.; Maccoll, A. *Can. J. Chem.* **1981**, *59*, 2228.
 (42) Klots, C. E. *J. Phys. Chem.* **1981**, *85*, 3585. Parsons, R. *Standard Potentials in Aqueous Solution*; Bard, A. J., Parsons, R., Jordan, J., Eds.; IUPAC Commissions on Electrochemistry and Electroanalytical Chemistry; M. Dekker: New York, 1985; p 13.
 (43) Lim, C.; Bashford, D.; Karplus, M. *J. Phys. Chem.* **1991**, *95*, 5610.

known experimental data. In calculating $\Delta G^{\circ}(\text{soln})$ for the neutral radicals from eq 8, the solution free energies are partitioned as the sum of hydrogen-bonding ($\Delta G^{\circ}(\text{HB})$) and non-hydrogen-bonding ($\Delta G^{\circ}(\text{NHB})$) terms, and the latter is treated as a constant which depends on the number of CH_2 units in the molecule. It was argued that the difference in $\Delta G^{\circ}(\text{soln})$ between α -carbon radicals, $R^1R^2NCR^3H^{\bullet}$, and the parent molecules, $R^1R^2NCR^3H_2$, is less than 2 kJ mol^{-1} and can be neglected. For the charged species, the difference between trimethylaminium ($(\text{CH}_3)_3\text{N}^{+\bullet}$) and trimethylammonium ($(\text{CH}_3)_3\text{NH}^+$) could be derived from experimental estimates of $\Delta G^{\circ}(\text{soln})$ of the two species. The increase in magnitude of the solution free energy of $(\text{CH}_3)_3\text{N}^{+\bullet}$ over that of $(\text{CH}_3)_3\text{NH}^+$ by 30 kJ mol^{-1} is assumed to apply in general to the $R^1R^2NCR^3H_2^{+\bullet}$ species and is used to derive heats of solution for the radical cations of methylamine, ethylamine, and dimethylamine. On the basis of the above analysis, the calculated values of $E^{\circ}_{(6)}$ for reaction 6 and $E^{\circ}_{(1)}$ for reaction 1 were very reasonable. The results confirmed the strong reducing character of the α -amino radicals.

Acknowledgment. The financial support of the Natural Sciences and Engineering Research Council of Canada is gratefully acknowledged.

Supplementary Material Available: MP2/6-31+G* optimized structures for H_2NCH_2^+ , $\text{H}_2\text{NCH}_2^{\bullet}$, H_2NCH_3 , $\text{H}_2\text{NCH}_3^{+\bullet}$, $\text{H}_3\text{NCH}_2^{+\bullet}$, $(\text{CH}_3)_2\text{NCH}_2^+$, $(\text{CH}_3)_2\text{NCH}_2^{\bullet}$, $(\text{CH}_3)_3\text{N}$, and $(\text{CH}_3)_3\text{N}^{+\bullet}$ (Table S-I), HF/6-31G* frequencies and infrared intensities for the above molecules (Table S-II), and ideal gas thermodynamic properties (Table S-III) (4 pages). Ordering information is given on any current masthead page.

An MC-SCF Study of the S_1 and S_2 Photochemical Reactions of Benzene

Ian J. Palmer,[†] Ioannis N. Ragazos,[†] Fernando Bernardi,^{*†} Massimo Olivucci,[†] and Michael A. Robb^{*†}

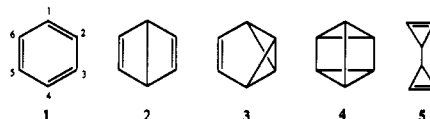
Contribution from the Dipartimento di Chimica "G. Ciamician" dell'Università di Bologna, Via Selmi 2, 40126 Bologna, Italy, and the Department of Chemistry, King's College London, Strand, London WC2R 2LS, U.K. Received July 16, 1992

Abstract: An MC-SCF/4-31G characterization of the possible photochemical pathways of S_1 and S_2 benzene is documented. A complete mechanistic scheme is presented through the characterization of minima and transition states on S_0 , S_1 , and S_2 . The full characterization of Born-Oppenheimer violation regions, where the products of the diabatic processes relax to lower electronic states, is also performed. On the S_0 surface the reversion of Dewar benzene to benzene is shown to occur via a concerted path along a symmetric coordinate where the bridgehead Dewar benzene bond and the pair of "quinoid" double bonds are being synchronously broken. No evidence for an asymmetric path could be found. The ground-state potential energy surface along the reaction path between benzene and benzvalene has a flat diradicaloid region corresponding to prefulvene. However, prefulvene itself is a transition state. The S_1 reaction path from benzene toward prefulvene contains an excited-state minimum with D_{6h} symmetry and a transition state between this minimum and a prefulvene diradicaloid located on the ground-state surface. The Born-Oppenheimer violation region has been fully characterized by optimizing the conical intersection that occurs between the transition state on S_1 and the prefulvene biradicaloid region on S_0 . The existence of a low-energy diradicaloid minimum on S_2 with an immediately adjacent S_1/S_2 conical intersection at only slightly higher energy has been demonstrated. This suggests that the radiationless decay from S_2 is almost completely efficient in contrast to the commonly held view. The different photochemistry of S_2 is shown to arise from the fact that the S_0/S_1 decay that occurs subsequent to passage through the S_1/S_2 conical intersection occurs at a geometry on the S_0/S_1 crossing surface where there is a $\text{C}_1\text{-C}_4$ bond similar in length to the bridgehead bond of the S_0 transition state between Dewar benzene and benzene. Thus there exists a ground-state reaction path to Dewar benzene from a high-energy region of the S_0/S_1 crossing surface.

Introduction

Photoexcitation of benzene permits the demise of the planar aromatic hexagonal ring system and movement along reaction coordinates toward the highly strained nonaromatic multiring valence isomers of benzene. The five observed valence isomers of benzene (Chart I) are the familiar Kekule form (1), Dewar

Chart I



benzene (2), benzvalene (3) (Huckel benzene), prismane (4) (Ladenburg benzene), and the bicyclic propenyl structure (5); all

[†] King's College London.

[†] Università di Bologna.